IOPscience iopscience.iop.org

Home Search Collections Journals About Contact us My IOPscience

Dust-acoustic shock waves in a strongly coupled dusty plasma with two-temperature nonthermal ions and transverse perturbations

This article has been downloaded from IOPscience. Please scroll down to see the full text article.

2006 J. Phys. A: Math. Gen. 39 7161

(http://iopscience.iop.org/0305-4470/39/22/025)

View the table of contents for this issue, or go to the journal homepage for more

Download details:
IP Address: 171.66.16.105
The article was downloaded on 03/06/2010 at 04:36

Please note that terms and conditions apply.

INSTITUTE OF PHYSICS PUBLISHING JOURNAL OF PHYSICS A: MATHEMATICAL AND GENERAL

J. Phys. A: Math. Gen. **39** (2006) 7161–7171 doi:10.1088/0305-4470/39/22/025

Dust-acoustic shock waves in a strongly coupled dusty plasma with two-temperature nonthermal ions and transverse perturbations

Yue-yue Wang[1] **and Jie-fang Zhang**[1,2]

[1] Institute of Nonlinear Physics, Zhejiang Normal University, Jinhua 321004, People's Republic of China
[2] CCAST (World Lab.), PO Box 8730, Beijing 10080, People's Republic of China

E-mail: jf_zhang@zjnu.cn

Received 23 November 2005, in final form 10 April 2006
Published 16 May 2006
Online at stacks.iop.org/JPhysA/39/7161

Abstract

In this paper, the nonlinear propagation of the dust-acoustic waves in a strongly coupled dusty plasma with two-temperature nonthermal ions and transverse perturbations is governed by a cylindrical Kadomtsev–Petviashvili–Burgers (KP–Burgers) equation. With the help of the variable-coefficient generalized projected Ricatti equation expansion method, the cylindrical KP–Burgers equation is solved and a shock wave solution is obtained. The effects on the amplitude of the shock wave caused by some important parameters such as ion nonthermal parameter a and temperature parameters β_1, β, etc are shown. The effects caused by dissipation and transverse perturbations are also discussed. It also indicates that the dust density hole can form and enlarge as time goes on.

PACS numbers: 52.35.Sb, 52.25.Vy, 05.45.Yv

1. Introduction

Since Rao, Shukla and Yu [1] theoretically predicted the existence of the dust-acoustic waves (DAW) in an unmagnetized dusty plasma, more and more people have investigated the linear and nonlinear features of the dust-acoustic waves [2–5]. A number of laboratory experiments have also verified that DAW can be observed even with naked eyes due to their appearance on a very long time scale [6, 7]. All these investigations give the properties of one-dimensional linear and nonlinear waves in a weakly coupled unmagnetized dusty plasma and they are well understood. However, the physics of strongly coupled plasmas is also of considerable interest because of its possible applications to white dwarf matter, interior of heavy planets, plasmas produced by laser compression of matter or in nuclear explosions and nonideal

 © 2006 IOP Publishing Ltd Printed in the UK

plasmas for industrial applications. In a strongly coupled dusty plasma, the intergrain spacing is of the order of the effective dusty plasma Debye radius and the electrostatic interaction energy of the shielded grains is much larger than the kinetic energy of the dust grains. Therefore, the coupling parameter Γ in a strongly coupled dusty plasma satisfies $\Gamma > 1$, and for $\Gamma > \Gamma_c$ (critical value) the dust grains form crystalline structures in the dusty plasma which supports a variety of dust lattice wave (DLW) modes [8], whereas for $1 \ll \Gamma < \Gamma_c$, the system is in a quasicrystal state; the system supports both longitudinal and transverse modes [9, 10].

Recently, a number of authors have considered the linear properties of DAW in a strongly coupled unmagnetized dusty plasma within the framework of either a generalized hydrodynamic (GH) model [11] or the quasi-localized charge (QLC) approximation [12], the local field correction (LFC) method [13]. Thereafter, the nonlinear properties of DAW in a strongly coupled unmagnetized dusty plasma have also been studied. For instance, Shukla and Stenflo [14] have shown that large-amplitude shear waves can excite vortex-like dust fluid motions in a strongly coupled dusty plasma and derived the governing equations for nonlinearly coupled transverse shear waves and zonal winds by employing the generalized hydrodynamic equations for the dust and Ampère's law. Shukla and Mamun [15] have investigated the properties of the shock wave structure in DAW in a strongly coupled unmagnetized dusty plasma and derived a Korteweg–de Vries–Burgers (KdV–Burgers) equation by the reductive perturbation technique on the GH equations, which admits shock solutions. Mamun *et al* [16] have derived the modified KdV–Burgers equation from a set of GH equations for strongly correlated grains in a liquid-like state, a Boltzmann electron distribution and a non-isothermal vortex-like ion distribution. They also give the numerical solutions of the modified KdV–Burgers equation to provide some salient features of dust-acoustic shock structures that exist in laboratory dusty plasmas. We extend the model mentioned in [16] and investigate the nonlinear propagation of DAW in strongly coupled plasmas with two-temperature nonthermal ions and transverse perturbations in a non-planar geometry. There are three reasons for us to study this model. First, observations of a space plasma indicate the presence of nonthermal ion populations. For instance, nonthermal ions have been observed in and around the Earth's foreshock [17]. The automatic space plasma experiment with a rotating analyser (ASPERA) on the Phobos satellite has detected nonthermal ion fluxes from the upper ionosphere of Mars [18]. Closer to the Earth, fast nonthermal ions have recently been observed by the Nozomi satellite in the vicinity of the Moon [19]. Therefore, an increasing interest is arising in investigating nonthermal ions in a dust plasma. Moreover, the negatively charged dust fluid and ions of two different temperatures (cold and hot) are the major plasma species in laboratory and space plasmas; therefore, the dusty plasmas with two-temperature nonthermal ions are much closer to the situation in real space. Second, many of those previous studies are limited to the one-dimensional geometry because it is easier and intuitional to study nonlinear waves in a dusty plasma bounded in the one-dimensional geometry; however, Franz *et al* [20] have shown that a purely one-dimensional model cannot account for all observed features in the auroral region, especially at higher polar altitudes. The transverse perturbations always exist in the higher dimensional system, and the wave structure deforms by the transverse perturbations. Therefore, it is necessary for us to take the weakly transverse perturbations into account. Finally, the results in [21–23] also indicate that the properties of solitary waves in a non-planar cylindrical/spherical geometry are very different from those in a planar geometry. Moreover, the waves observed in laboratory devices are certainly not bounded in a planar geometry but are usually bounded in a non-planar geometry. Summing up all these reasons, we study the DAW in a strongly dusty plasma with two-temperature nonthermal ions and

transverse perturbations in a cylindrical geometry but neglect the dust-neutral collision due to the conclusion obtained by [24] in which they point out that the dust-neutral collision does not appear to play any direct role in shock formation. Further, we obtain the analytical solution by symbolic computation and analyse the effects on the amplitude of the dust-acoustic shock wave caused by different parameters and transverse perturbations as well as the non-planar geometry.

The paper is organized as follows. In section 2, we present the GH equations governing the dynamics of the nonlinear DAW consisting of two-temperature nonthermal ions and adiabatic variational charged dust grains for the strongly coupled dusty plasma. We derive the cylindrical KP–Burgers equation by means of the reductive perturbation technique in section 3. In section 4, we give the shock wave solution and discuss the effects caused by nonthermal ions, transverse perturbations and dissipation. Finally, a conclusion is presented in section 5.

2. Governing equations

We study the dust-acoustic waves (DAW) in the non-planar cylindrical geometry for an unmagnetized strongly coupled dusty plasma with transverse perturbations. We also assume that electrons and ions are weakly coupled due to their higher temperatures and smaller electric charges, compared to the dust grains. The electrons' number density obeys the Boltzmann law, while the ions are assumed to be nonthermally distributed. Due to the lower temperature and larger electric charge, the dust grains are assumed to be strongly coupled. Considering the transverse perturbations, the dynamics of the DAW in a strongly coupled dusty plasma can be investigated by means of the well-known GH equations normalized as follows:

$$\begin{cases} \dfrac{\partial n_{\mathrm{d}}}{\partial t} + \dfrac{1}{r}\dfrac{\partial (r n_{\mathrm{d}} u_{\mathrm{d}})}{\partial r} + \dfrac{1}{r}\dfrac{\partial (n_{\mathrm{d}} v_{\mathrm{d}})}{\partial \theta} = 0, \\ \left(1 + \tau_{\mathrm{m}} \dfrac{\partial}{\partial t}\right)\left[n_{\mathrm{d}} \left(\dfrac{\partial u_{\mathrm{d}}}{\partial t} + u_{\mathrm{d}} \dfrac{\partial u_{\mathrm{d}}}{\partial r} + \dfrac{v_{\mathrm{d}}}{r}\dfrac{\partial u_{\mathrm{d}}}{\partial \theta} - \dfrac{v_{\mathrm{d}}^2}{r} - Z_{\mathrm{d}} \dfrac{\partial \phi}{\partial r} \right)\right] \\ \quad = \eta_{\mathrm{l}} \left[\dfrac{1}{r}\dfrac{\partial}{\partial r}\left(r \dfrac{\partial u_{\mathrm{d}}}{\partial r}\right) + \dfrac{1}{r^2}\dfrac{\partial^2 u_{\mathrm{d}}}{\partial \theta^2} - \dfrac{1}{r^2}\left(u_{\mathrm{d}} + 2\dfrac{\partial v_{\mathrm{d}}}{\partial \theta}\right)\right], \\ \left(1 + \tau_{\mathrm{m}} \dfrac{\partial}{\partial t}\right)\left[n_{\mathrm{d}} \left(\dfrac{\partial v_{\mathrm{d}}}{\partial t} + u_{\mathrm{d}} \dfrac{\partial v_{\mathrm{d}}}{\partial r} + \dfrac{v_{\mathrm{d}}}{r}\dfrac{\partial v_{\mathrm{d}}}{\partial \theta} + \dfrac{v_{\mathrm{d}} u_{\mathrm{d}}}{r} - Z_{\mathrm{d}} \dfrac{1}{r}\dfrac{\partial \phi}{\partial \theta} \right)\right] \\ \quad = \eta_{\mathrm{l}} \left[\dfrac{1}{r}\dfrac{\partial}{\partial r}\left(r \dfrac{\partial v_{\mathrm{d}}}{\partial r}\right) + \dfrac{1}{r^2}\dfrac{\partial^2 v_{\mathrm{d}}}{\partial \theta^2} - \dfrac{1}{r^2}\left(v_{\mathrm{d}} - 2\dfrac{\partial u_{\mathrm{d}}}{\partial \theta}\right)\right], \\ \dfrac{1}{r}\dfrac{\partial}{\partial r}\left(r \dfrac{\partial \phi}{\partial r}\right) + \dfrac{1}{r^2}\dfrac{\partial^2 \phi}{\partial \theta^2} = Z_{\mathrm{d}} n_{\mathrm{d}} + n_{\mathrm{e}} - n_{\mathrm{il}} - n_{\mathrm{ih}}, \end{cases} \tag{1}$$

where u_{d} and v_{d} represent the velocity components of the dust particles in the radial and polar angle directions, i.e. r and θ directions; they are normalized by the effective dust-acoustic speed $C_{\mathrm{d}} = \sqrt{\frac{Z_{\mathrm{d0}} T_{\mathrm{eff}}}{m_{\mathrm{d}}}}$. The space variables are normalized by the Debye length $\lambda_{\mathrm{Dd}} = \sqrt{\frac{T_{\mathrm{eff}}}{4\pi e^2 n_{\mathrm{d0}} Z_{\mathrm{d0}}}}$. n_{d} represents the dust density and Z_{d} refers to the number of charges residing on the dust grain surface. ϕ represents the electrostatic wave potential normalized by T_{eff}/e. τ_{m} refers to the viscoelastic relaxation time normalized by the dust plasma period $\omega_{\mathrm{pd}}^{-1} = \sqrt{\frac{m_{\mathrm{d}}}{4\pi n_{\mathrm{d0}} Z_{\mathrm{d0}}^2 e^2}}$ given as

$$\tau_{\mathrm{m}} = \eta_{\mathrm{l}} \frac{T_{\mathrm{e}}}{T_{\mathrm{d}}} \left[1 - \mu_{\mathrm{d}} + \frac{4}{15} u(\Gamma) \right]^{-1}, \tag{2}$$

where

$$\mu_{\mathrm{d}} = 1 + \frac{1}{3}u(\Gamma) + \frac{\Gamma}{9}\frac{\partial u(\Gamma)}{\partial \Gamma} \tag{3}$$

is the compressibility [25], $u(\Gamma) = E_{\mathrm{c}}/(n_{\mathrm{d}0}T_{\mathrm{d}})$ is a measure of the excess internal energy of the system and E_{c} is the correlation energy. For weakly coupled plasmas $(\Gamma \ll 1), u(\Gamma) \approx -(\sqrt{3}/2)\Gamma^{3/2}$, whereas in the range $1 \leqslant \Gamma \leqslant 200$, Slattery *et al* have analytically derived a relation $u(\Gamma) \approx 0.89\Gamma + 0.95\Gamma^{1/4} + 0.19\Gamma^{-1/4} - 0.81$ [26], where a small correction term due to finite number of particles is neglected. η_{l} is the normalized viscosity coefficient given as

$$\eta_{\mathrm{l}} = \frac{1}{m_{\mathrm{d}} n_{\mathrm{d}0}\omega_{\mathrm{pd}}\lambda_{\mathrm{Dd}}^2}\left[\eta_{\mathrm{b}} + \frac{4}{3}\zeta_{\mathrm{b}}\right], \tag{4}$$

where η_{b} and ζ_{b} are transport coefficients of shear and bulk viscosities.

The normalized density of the Boltzmann distributed electron and two-temperature nonthermally distributed ions $n_{\mathrm{e}}, n_{\mathrm{il}}$ and n_{ih} is given by

$$\begin{cases} n_{\mathrm{e}} = \nu\, \mathrm{e}^{(s\beta_1\phi)}, \\ n_{\mathrm{il}} = \mu_1\left[1 + \dfrac{4a}{1+3a}(s\phi + s^2\phi^2)\right]\mathrm{e}^{(-s\phi)}, \\ n_{\mathrm{ih}} = \mu_{\mathrm{h}}\left[1 + \dfrac{4a}{1+3a}(\beta s\phi + \beta^2 s^2\phi^2)\right]\mathrm{e}^{(-\beta s\phi)}, \end{cases} \tag{5}$$

where n_{e} refers to electrons with temperature T_{e} and equilibrium density ν, n_{il} refers to ions with low temperature T_{il} and equilibrium density μ_1, and n_{ih} refers to ions with high temperature T_{ih} and equilibrium density μ_{h}, where $\nu = \frac{n_{\mathrm{e}0}}{Z_{\mathrm{d}0}n_{\mathrm{d}0}}$, $\mu_1 = \frac{n_{\mathrm{il}0}}{Z_{\mathrm{d}0}n_{\mathrm{d}0}}$, $\mu_{\mathrm{h}} = \frac{n_{\mathrm{ih}0}}{Z_{\mathrm{d}0}n_{\mathrm{d}0}}$. The equilibrium condition is $n_{\mathrm{il}0} + n_{\mathrm{ih}0} = n_{\mathrm{e}0} + Z_{\mathrm{d}}n_{\mathrm{d}0}$, in which $n_{\mathrm{i}0}, n_{\mathrm{d}0}$ and $n_{\mathrm{e}0}$ are the unperturbed ion, dust and electron number densities, respectively. As the ions are assumed to be nonthermally distributed, the two-temperature ions' density can be obtained by the same way as introduced in [24]. In equation (5), a is the ion nonthermal parameter which determines the number of fast ions. The nonthermally distributed ion density will reduce to the Boltzmann distribution when $a = 0$. The other parameters are chosen as $\beta_1 = \frac{T_{\mathrm{il}}}{T_{\mathrm{e}}}, \beta = \frac{T_{\mathrm{il}}}{T_{\mathrm{ih}}}, s = \frac{T_{\mathrm{eff}}}{T_{\mathrm{il}}}, \frac{1}{T_{\mathrm{eff}}} = \frac{1}{Z_{\mathrm{d}}n_{\mathrm{d}0}}\left(\frac{n_{\mathrm{e}0}}{T_{\mathrm{e}}} + \frac{n_{\mathrm{il}0}}{T_{\mathrm{il}}} + \frac{n_{\mathrm{ih}0}}{T_{\mathrm{ih}}}\right)$.

On the other hand, it worth noting that the dust charging time is $\sim 10^{-9}$ s, while the dust motion time is $\sim 10^{-3}$ s. Thus, the dust charge can quickly reach to the local equilibrium at which the currents from the electrons and ions to the dust are balanced [28]. The current balance equation reads

$$I_{\mathrm{e}} + I_{\mathrm{il}} + I_{\mathrm{ih}} \approx 0, \tag{6}$$

where the electron grain current can be obtained as follows:

$$I_{\mathrm{e}} = -e\pi r^2\sqrt{\frac{8T_{\mathrm{e}}}{\pi m_{\mathrm{e}}}}\nu \exp\left(s\beta_1\phi + \frac{e\phi}{T_{\mathrm{e}}}\right), \tag{7}$$

while the two-temperature nonthermally distributed ions' currents to dust grains can be obtained by means of the orbital-motion-limited (OML) approach

$$I_{\mathrm{il}} = e\pi r^2\sqrt{\frac{8T_{\mathrm{il}}}{\pi m_{\mathrm{i}}}}\frac{\mu_1}{1+3a}\exp(-s\phi)\left[\left(1 + \frac{24a}{5} + \frac{16a}{3}s\phi + 4as^2\phi^2\right)\right.$$
$$\left. - s\psi\left(1 + \frac{8a}{5} + \frac{8a}{3}s\phi + 4as^2\phi^2\right)\right],$$

$$I_{\rm ih} = e\pi r^2 \sqrt{\frac{8T_{\rm ih}}{\pi m_{\rm i}}} \frac{\mu_{\rm h}}{1+3a} \exp(-s\beta\phi) \left[\left(1 + \frac{24a}{5} + \frac{16a}{3} s\beta\phi + 4as^2\beta^2\phi^2 \right) - s\beta\psi \left(1 + \frac{8a}{5} + \frac{8a}{3} s\beta\phi + 4as^2\beta^2\phi^2 \right) \right], \tag{8}$$

where r is the spherical dust grain of average radius.

3. Derivation of the cylindrical KP–Burgers equation

The reductive perturbation technique (RPT) is a well-known method mostly applied to small-amplitude nonlinear waves. We apply this technique to derive the cylindrical Kadomtsev–Petviashvili–Burgers (KP–Burgers) equation for small-amplitude DAW in a strongly coupled dusty plasma with transverse perturbations. We choose the stretched coordinates $\xi = \epsilon^{1/2}(r - ct)$, $\eta = \epsilon^{-1/2}\theta$, $\tau = \epsilon^{3/2}t$, $\eta_{\rm l} = \epsilon^{1/2}\eta_0$, $\tau_{\rm m} = \epsilon^{1/2}\tau_{\rm m0}$. We expand the dependent variables about their equilibrium values in powers of ϵ as

$$\begin{cases} n_{\rm d} = 1 + \epsilon n_{\rm d1} + \epsilon^2 n_{\rm d2} + \epsilon^3 n_{\rm d3} + \cdots, \\ u_{\rm d} = \epsilon u_{\rm d1} + \epsilon^2 u_{\rm d2} + \epsilon^3 u_{\rm d3} + \cdots, \\ \phi = \epsilon\phi_1 + \epsilon^2\phi_2 + \epsilon^3\phi_3 + \cdots, \\ v_{\rm d} = \epsilon^{\frac{3}{2}} v_{\rm d1} + \epsilon^{\frac{5}{2}} v_{\rm d2} + \epsilon^{\frac{7}{2}} v_{\rm d3} + \cdots, \\ Z_{\rm d} = 1 + \epsilon Z_{\rm d1} + \epsilon^2 Z_{\rm d2} + \epsilon^3 Z_{\rm d3} + \cdots. \end{cases} \tag{9}$$

Substituting equations (5)–(9) into equation (1) and collecting the terms in different powers of ϵ, we obtain the following equations of the lowest order in ϵ:

$$\begin{cases} \nu = \mu_{\rm l} + \mu_{\rm h} - 1, \\ n_{\rm d1} = -\dfrac{\phi_1}{c^2}, \\ u_{\rm d1} = -\dfrac{\phi_1}{c}, \\ \dfrac{\partial v_{\rm d1}}{\partial \xi} = -\dfrac{1}{c^2\tau} \dfrac{\partial \phi_1}{\partial \eta}, \\ Z_{\rm d1} = \gamma_1 \phi_1, \end{cases} \tag{10}$$

where $c^2 = \frac{1}{(\nu s\beta_1 + \mu_{\rm h}\beta s + \gamma_1 - \mu_{\rm l}\alpha s - \mu_{\rm h}\alpha s\beta + \mu_{\rm l} s)}$ and $\gamma_1 = \frac{\gamma_{1a}}{\gamma_{1b}}$, while

$$\begin{aligned} \gamma_{1a} &= -[(-72a + 24s\psi_0 a + 15s\psi_0 - 15)\beta_1 - 15 + 8a + 15s\psi_0 - 16s\psi_0 a]\delta_1 \\ &\quad - [(-15 - 72a + 15\psi_0\beta s + 24\psi_0\beta sa)\beta_1 - \beta(16\psi_0\beta sa - 15\psi_0\beta s - 8a + 15)]\delta_2, \\ \gamma_{1b} &= 3\psi_0\delta_1[(8s\psi_0 a - 5 + 5s\psi_0 - 24a)\beta_1 - 5 - 8a] \\ &\quad + 3\psi_0\delta_2[(5\psi_0\beta s - 5 + 8\psi_0\beta sa - 24a)\beta_1 - \beta(5 + 8a)], \end{aligned}$$

in which $\alpha = \frac{4a}{(1+3a)}$, $\delta_1 = \frac{n_{\rm il0}}{n_{\rm e0}}\sqrt{\frac{T_{\rm il}}{T_{\rm e}\mu_{\rm i}}}$, $\delta_2 = \frac{n_{\rm ih0}}{n_{\rm e0}}\sqrt{\frac{T_{\rm ih}}{T_{\rm e}\mu_{\rm i}}}$ with the ion-to-electron mass ratio $\mu_{\rm i} = \frac{m_{\rm i}}{m_{\rm e}} \simeq 1840$, and ψ_0 satisfies the relation

$$\exp(\beta_1 s\psi_0) = \frac{\delta_1}{1+3a}\left[1 + \frac{24a}{5} - s\psi_0\left(1 + \frac{8a}{5}\right)\right] + \frac{\delta_2}{1+3a}\left[1 + \frac{24a}{5} - s\beta\psi_0\left(1 + \frac{8a}{5}\right)\right].$$

The next order of ϵ gives

$$\begin{cases} c\tau\dfrac{\partial n_{\mathrm{d}1}}{\partial\tau}+u_{\mathrm{d}1}+c\tau\dfrac{\partial u_{\mathrm{d}2}}{\partial\xi}-c^2\tau\dfrac{\partial n_{\mathrm{d}2}}{\partial\xi}+c\tau\dfrac{\partial n_{\mathrm{d}1}}{\partial\xi}u_{\mathrm{d}1}+\dfrac{\partial v_{\mathrm{d}1}}{\partial\eta}+c\tau n_{\mathrm{d}1}\dfrac{\partial u_{\mathrm{d}1}}{\partial\xi}=0, \\ c^2\tau^2\dfrac{\partial u_{\mathrm{d}1}}{\partial\tau}+c^2\tau^2u_{\mathrm{d}1}\dfrac{\partial u_{\mathrm{d}1}}{\partial\xi}-c^3\tau^2\dfrac{\partial u_{\mathrm{d}2}}{\partial\xi}-\eta_0c^2\tau^2\dfrac{\partial^2u_{\mathrm{d}1}}{\partial\xi^2}-c^2\tau^2\gamma_1\phi_1\dfrac{\partial\phi_1}{\partial\xi} \\ \quad -c^2\tau^2\dfrac{\partial\phi_2}{\partial\xi}+\tau_{\mathrm{m}0}c^3\tau^2\dfrac{\partial^2\phi_1}{\partial\xi^2}+\tau_{\mathrm{m}0}c^4\tau^2\dfrac{\partial^2u_{\mathrm{d}1}}{\partial\xi^2}-c^3\tau^2n_{\mathrm{d}1}\dfrac{\partial u_{\mathrm{d}1}}{\partial\xi}-c^2\tau^2n_{\mathrm{d}1}\dfrac{\partial\phi_1}{\partial\xi}=0, \\ -\dfrac{1}{2}\nu c^2\tau^2\beta_1^2s^2\phi_1^2+\tau^2\nu s\big(-\phi_2+\phi_1^2\gamma_1\big)c^2\beta_1+\dfrac{1}{2}\tau^2\phi_1^2(\beta^2\mu_{\mathrm{h}}+\mu_1)c^2s^2 \\ \quad -\tau^2\big(-\phi_2+\phi_1^2\gamma_1\big)(\alpha-1)(\mu_1+\beta\mu_{\mathrm{h}})c^2s \\ \quad +c^2\tau^2\left(\dfrac{\partial^2\phi_1}{\partial\xi^2}+\phi_1^2\gamma_1^2-\gamma_2\phi_1^2-\gamma_1\phi_2-n_{\mathrm{d}2}\right)=0, \\ Z_{\mathrm{d}2}=\gamma_2\phi_1^2+\gamma_1\phi_2, \end{cases} \tag{11}$$

where γ_1 was mentioned above and

$$\gamma_2=\frac{\gamma_{2a}}{\gamma_{2b}},$$

in which

$$\begin{aligned} \gamma_{2a}=&-s\delta_1\big\{\big[3\psi_0^2\gamma_1^2(8s\psi_0a-5+5s\psi_0-24a)+6\psi_0\gamma_1(8s\psi_0a-5+5s\psi_0-24a)-72a \\ &+24s\psi_0a+15s\psi_0-15\big]\beta_1^2-2\psi_0(-15+16a)\gamma_1+15-15s\psi_0+32a \\ &-64s\psi_0a\big\}-s\delta_2\big\{\big[3\psi_0^2(5\psi_0\beta s-5+8\psi_0\beta sa-24a)\gamma_1^2+6\psi_0(5\psi_0\beta s-5 \\ &+8\psi_0\beta sa-24a)\gamma_1-15-72a+15\psi_0\beta s+24\psi_0\beta sa\big]\beta_1^2 \\ &-2\beta^2\psi_0\gamma_1(-15+16a)-\beta^2(15\psi_0\beta s+64\psi_0\beta sa-15-32a)\big\}, \\ \gamma_{2b}=&\,6\psi_0\delta_1[(8s\psi_0a-5+5s\psi_0-24a)\beta_1-5-8a] \\ &+6\psi_0\delta_2[(5\psi_0\beta s-5+8\psi_0\beta sa-24a)\beta_1-\beta(5+8a)]. \end{aligned}$$

If we set $a=0$, γ_1 and γ_2 are consistent with those in [29] where the two-temperature ions are Boltzmann distributed. In this paper, we have investigated the dust grains with adiabatic dust charge variation. If γ_1, γ_2 reduce to zero, then $Z_{\mathrm{d}}=1$, corresponding to the no dust charge variation.

Substituting equation (10) into equation (11) yields a cylindrical KP–Burgers equation:

$$\frac{\partial}{\partial\xi}\left[\frac{\partial\phi_1}{\partial\tau}+\frac{\phi_1}{2\tau}+A\phi_1\frac{\partial\phi_1}{\partial\xi}+B\frac{\partial^3\phi_1}{\partial\xi^3}-\frac{1}{2}\eta_0\frac{\partial^2\phi_1}{\partial\xi^2}\right]+\frac{1}{2c\tau^2}\frac{\partial^2\phi_1}{\partial\eta^2}=0, \tag{12}$$

where $A=\frac{1}{2}\big(\beta^2\mu_{\mathrm{h}}-\nu\beta_1^2+\mu_1\big)c^3s^2-\gamma_1(-\nu\beta_1-\beta\mu_{\mathrm{h}}+\beta\alpha\mu_{\mathrm{h}}-\mu_1+\alpha\mu_1)c^3s+\big(\gamma_1^2-\gamma_2\big)c^3+\frac{\gamma_1c}{2}-\frac{3}{2c}$ and $B=\frac{c^3}{2}$.

It is clear that the adiabatic dust charge variation only affects the nonlinear term and the dispersive term but has no effect on the transverse perturbations' term and the dissipative term. It is worth noting that equation (12) does not contain the effect of $\tau_{\mathrm{m}0}$ because the terms containing $\tau_{\mathrm{m}0}$ vanish or drop out. Therefore, $\tau_{\mathrm{m}0}$ has nothing to do with the formation of shock wave structure. As long as the dispersive term and the dissipative term as well as the nonlinear term are balanced, the shock wave structure forms; otherwise, the soliton forms due to the balance between the dispersive term and the nonlinear term. Therefore, from equation (12), we can see that the dust viscosity through dust–dust correlation will cause the dissipation which finally determines the formation of shock wave structure.

If the transverse perturbations are neglected, the cylindrical KP–Burgers equation degenerates into the cylindrical KdV–Burgers equation:

$$\frac{\partial\phi_1}{\partial\tau}+\frac{\phi_1}{2\tau}+A\phi_1\frac{\partial\phi_1}{\partial\xi}+B\frac{\partial^3\phi_1}{\partial\xi^3}-\frac{1}{2}\eta_0\frac{\partial^2\phi_1}{\partial\xi^2}=0. \tag{13}$$

It is still different from the KdV–Burgers equation derived by previous works [15, 16] because we investigate this in the non-planar geometry instead of the planar geometry.

4. Shock wave solution and analysis of the effects caused by nonthermal ions, transverse perturbations and dissipation

To the best of our knowledge, the dust-acoustic shock waves in a strongly coupled dusty plasma are investigated by numerical calculation in previous papers. However, it seems that the analytical solution is more accurate than the numerical calculation because the latter always induces an error. Therefore, at present, many new methods are introduced to obtain the analytical solutions for various equations. It seems that the generalized projected Ricatti equation expansion method [30] is one of the most effective methods to obtain the analytical solutions for the variable-coefficient equation. By using this method, we can easily obtain several analytical solutions for equation (12), such as solitary wave solutions, singularity solitary wave solutions and triangular function solutions. However, considering that the singularity solitary wave solutions and triangular function solutions are meaningless in a dusty plasma, we present only the most typical shock wave solution:

$$\begin{aligned}\phi_1=&-\frac{20B\sqrt{R}}{\eta_0 A}\frac{\eta\,\mathrm{d}\alpha_1(\tau)}{\mathrm{d}\tau}-\frac{20B\sqrt{R}}{\eta_0 A}\frac{\mathrm{d}\alpha_2(\tau)}{\mathrm{d}\tau}+\frac{20\sqrt{R}B\eta\alpha_1(\tau)}{\eta_0\tau A}-\frac{200RB^2\alpha_1^2(\tau)}{\eta_0^2 c\tau^2 A}\\&-\frac{3\eta_0^2}{50BA}\tanh\left[\sqrt{R}\left(\frac{\eta_0}{20B\sqrt{R}}\xi-\frac{\eta_0 c\tau\eta^2}{40B\sqrt{R}}+\alpha_1(\tau)\eta+\alpha_2(\tau)\right)\right]\\&+\frac{3\eta_0^2}{100BA}\mathrm{sech}^2\left[\sqrt{R}\left(\frac{\eta_0}{20B\sqrt{R}}\xi-\frac{\eta_0 c\tau\eta^2}{40B\sqrt{R}}+\alpha_1(\tau)\eta+\alpha_2(\tau)\right)\right],\end{aligned} \tag{14}$$

where R is an arbitrary constant with $R\geqslant 0$, $\alpha_1(\tau)$ and $\alpha_2(\tau)$ can be chosen as arbitrary functions varying with τ. A and B are the same as mentioned above.

In the following, according to the figures for the shock wave solution (equation (14)), we analyse the effects of the plasma parameters such as ion nonthermal parameter a, β_1 and β, etc. The effects of transverse perturbations and dissipation caused by dust viscosity through dust–dust correlation are also discussed.

It indicates that the ion nonthermal parameter a not only affects the normalized dust charges Z_d but also affects the amplitude (ϕ) of shock wave structures. When $a=0$, Z_d and ϕ correspond to those of the DAW in the strongly coupled plasma containing two-temperature Boltzmann distributed ions. When the nonthermal ions exist, the amplitude enlarges and the shock wave structure becomes steeper. Further, when the ion nonthermal parameter a exceeds the critical value a^*, the shock wave structure changes from a kink wave structure to an anti-kink wave structure; after that, the amplitude decreases as the parameter a increases (see figure 1(a)). According to the solution (equation (14)), the shock wave structure is a kink wave structure or an anti-kink wave structure depends mainly on the sign of the product of the coefficient of the nonlinear term and the dispersion term, that is, $AB>0$ or $AB<0$ in equation (14). When $AB<0$, a kink wave structure is present, otherwise, namely $AB>0$, an anti-kink wave structure is present. Therefore, the critical value a^* can be determined by

$$\begin{aligned}&-2c^4\gamma_1^2+[2\mu_\mathrm{h}sc^4\beta(-1+\alpha)-2sc^4(\nu\beta_1-\mu_1\alpha+\mu_1)-c^2]\gamma_1\\&\qquad-c^4\mu_\mathrm{h}\beta^2s^2+3+\left(\nu\beta_1^2s^2-\mu_1s^2+2\gamma_2\right)c^4=0.\end{aligned}$$

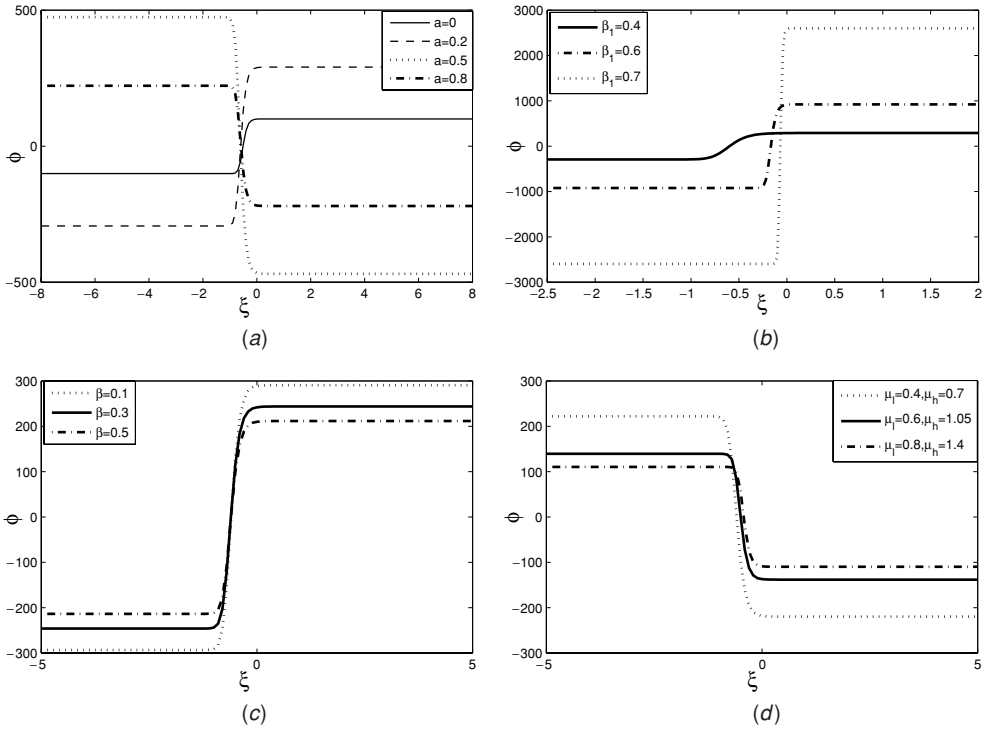

Figure 1. (*a*) The potential ϕ against ξ with parameters $\beta = 0.1$, $\beta_1 = 0.4$, $\mu_1 = 0.4$, $\mu_h = 0.7$ for different values of a. Panel (*b*) shows the potential ϕ against ξ with parameters $a = 0.2$, $\beta = 0.1$, $\mu_1 = 0.4$, $\mu_h = 0.7$ for different values of β_1. Panel (*c*) shows the potential ϕ against ξ with parameters $a = 0.2$, $\beta_1 = 0.4$, $\mu_1 = 0.4$, $\mu_h = 0.7$ for different values of β. Panel (*d*) shows the potential ϕ against ξ with parameters $a = 0.2$, $\beta = 0.1$, $\beta_1 = 0.4$ for different values of μ_1 and μ_h. The common parameters for (*a*)–(*d*) are $\eta_0 = 10$, $R = 10$, $\alpha_1(\tau) = \sin(\tau)$, $\alpha_2(\tau) = \sin(\tau)$, $\delta_1 = 12$, $\delta_2 = 8$, $\tau = 2$, $\eta = 0.1$.

The case containing only one-temperature ions in the dusty plasmas is quite different from the case containing both the cold and hot ions because they will affect the amplitude of the shock wave structure. Thus, we investigate the effect of the temperature and density of the two-temperature ions and find that not only the temperature parameters of the cold and hot ions (β_1 and β) but also the density will affect the amplitude of the shock wave structure. The amplitude increases as β_1 increases (figure 1(*b*)) but decreases as β increases (figure 1(*c*)). Because μ_1 and μ_h are in direct proportion to unperturbed ions' density (n_{il0} and n_{ih0}), increasing n_{il0} and n_{ih0} will cause the increase of μ_1 and μ_h. It indicates that the amplitudes of shock wave structures decrease as n_{il0} and n_{ih0} increase (figure 1(*d*)). From above figures, we can draw a conclusion that the magnitude of the amplitude will be affected by the ion nonthermal parameter a, temperature parameters of cold and hot ions β_1 and β, and the unperturbed density of hot and cold ions, but has nothing to do with the transverse perturbations.

From figures 2(*a*) and (*b*), it is clear that although the transverse perturbations will not increase or decrease the amplitude, however, they deform the shock wave structure and change it into a nonstandard one. When the transverse perturbations become larger and cannot be neglected, then the shock wave structure deforms and forms a parabolic shock wave structure. Then we plot the evolution figures of the dust density n_d (figure 2(*c*)) by transforming the coordinates (ξ, η, τ) back to the cylindrical coordinates (r, θ, t), and then correspondingly to

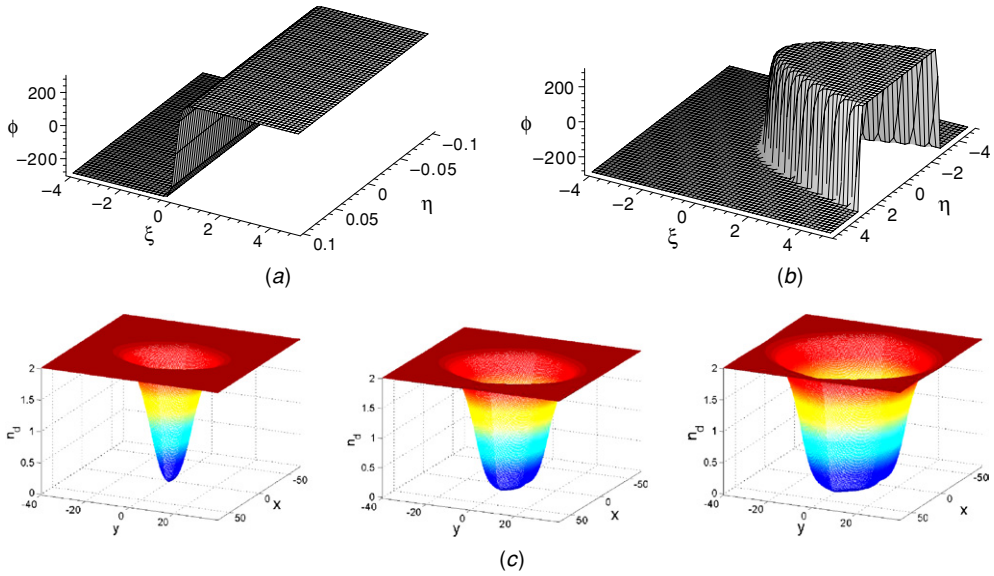

Figure 2. Panels (a) and (b) show the shock wave structure with smaller values of η and larger values of η; the common parameters are $a = 0.2, \eta_0 = 10, R = 10, \alpha_1(\tau) = 0, \alpha_2(\tau) = 0, \delta_1 = 12, \delta_2 = 8, \tau = 2, \beta = 0.1, \beta_1 = 0.4$. ($c$) The evolution figures ($t = 10 \longrightarrow t = 20 \longrightarrow t = 30$) of dust density in Cartesian coordinates (x, y) with $\epsilon = 0.0008, R = 20, \eta_0 = 10, a = 0.5, \beta = 0.1, \beta_1 = 0.4, \mu_1 = 0.4, \mu_h = 0.7, \alpha_1(\tau) = 0, \alpha_2(\tau) = 0, \delta_1 = 12, \delta_2 = 8$.

(This figure is in colour only in the electronic version)

the Cartesian coordinates (x, y, t). It is because the Cartesian coordinates are the reference frame that experiments in general tend to consider. We find that there exists a dust density hole which is similar to the dust void. As time goes on, the dust density hole is enlarged. So far, the dust void has been observed in laboratory plasmas; we hope that the present investigation would be helpful for the future experiment and observation in strong coupled dusty plasmas and this phenomenon can be verified in laboratory plasmas in the future. The dust density holes can be formed due to the effect of transverse perturbations and the effect caused by the non-planar geometry. Therefore, we cannot find the same structure in the one-dimensional planar geometry when the transverse perturbation is neglected.

Finally, we investigate the evolution figures of the shock wave structure. The shock wave solution (equation (14)), which is obtained by means of the generalized projected Ricatti equation expansion method, depends on the parameters $\alpha_1(\tau)$ and $\alpha_2(\tau)$ which can be chosen as arbitrary functions. If α_1 and α_2 are large enough, the forms of α_1 and α_2 significantly affect the evolution figure of the shock wave solution. For instance, if we choose α_1 as sinusoid, it is clear that the kink wave structure moves up and down along a route of sinusoid as time goes on (figure 3(a)). If we set $\alpha_1 = 0$ and $\alpha_2 = 0$, then the shock wave structure remains stable as time goes on. Figure 3(b) shows the effect of dissipation. As the dissipation depends mainly on the parameter η_0, we study the variation of amplitude with respect to η_0 and find that the amplitude of the shock wave structure increases as η_0 increases, and the shock wave structure becomes steeper. If the dissipation is neglected, the shock wave structure no longer exists due to the break of the balance among the dispersive term, the nonlinear term and the dissipative term, and a new balance between the dispersive term and the nonlinear term will form which admits the existence of the soliton structure.

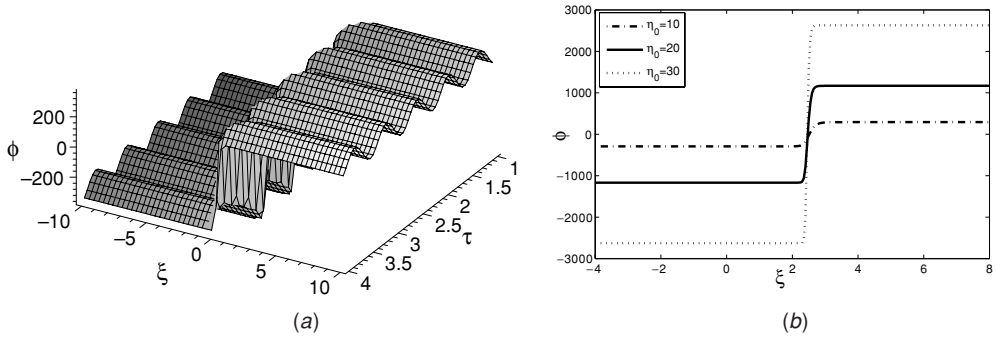

Figure 3. (*a*) The evolution figure of the shock wave structure with parameters $a = 0.2$, $\beta = 0.1$, $\beta_1 = 0.4$, $\mu_1 = 0.4$, $\mu_h = 0.7$, $\eta_0 = 10$, $R = 10, \alpha_1(\tau) = \sin(10\tau), \alpha_2(\tau) = \sin(10\tau)$, $\delta_1 = 12, \delta_2 = 8$. (*b*) The potential ϕ against ξ with parameters $a = 0.2, \beta = 0.1, \beta_1 = 0.4$, $\mu_1 = 0.4, \mu_h = 0.7, R = 10, \alpha_1(\tau) = 0, \alpha_2(\tau) = 0, \delta_1 = 12, \delta_2 = 8, \eta = 2, \tau = 5$ for different values of η_0.

5. Conclusion

In this paper, the cylindrical KP–Burgers equation, which describes the nonlinear propagation of DAW in a strongly coupled dusty plasma with two-temperature nonthermal distributed ions and transverse perturbations, has been successfully derived. Instead of obtaining the numerical solutions, we give the analytical solution which is a shock wave solution. According to the evolution figures, we can draw a conclusion that the amplitude of the shock wave is affected by ion nonthermal parameter a, temperature parameters β_1, β and the density of the two-temperature ions; that is, ϕ increases as a, β_1 and n_{il0}, n_{ih0} increase, while decreases as β increases. The dissipation caused by the dust viscosity through dust–dust correlation also has an effect on the amplitude of the shock wave. With the stronger dissipation, the shock wave structure becomes steeper and the electrostatic potential (ϕ) becomes higher. If the dissipation is neglected, the shock wave structure no longer exists due to the break of the balance among the dispersive term, the nonlinear term and the dissipative term. The shock wave evolution figures also depend on α_1 and α_2. As long as α_1 and α_2 are chosen as a certain function, the shock wave will propagate according to this function. It is worth noting that if $a = 0$ is satisfied, then the dust charge number Z_d will reduce to the case where the plasmas are containing the two-temperature Boltzmann distributed ions, while $\gamma_1 = 0$ and $\gamma_2 = 0$ are satisfied, then it reduces to the case of no dust charge variation. It also indicates that the shock wave structure will deform due to the transverse perturbations. If the transverse perturbations are neglected, i.e. $\eta = 0$, then the shock wave structure is standard shaped and the propagation of the shock wave is stable. Transforming the coordinates (ξ, η, τ) back to Cartesian coordinates (x, y, t), we have found that there exists a dust hole and it will enlarge as times goes on. The purpose of studying the transverse perturbations and dissipative effects of the dust-acoustic shock wave in a non-planar strongly coupled plasma is to gain understanding on the propagation characteristics of the dust-acoustic shock wave that are of vital importance in the laboratory plasma as well as in the space plasma which are strongly coupled.

References

[1] Rao N N, Shukla P K and Yu M Y 1990 *Planet. Space Sci.* **38** 543
[2] Rao N N and Shukla P K 1994 *Planet. Space Sci.* **42** 221

[3] Melandsø F and Shukla P K 1995 *Planet. Space Sci.* **43** 635
[4] Shukla P K and Mamun A A 2002 *Introduction to Dusty Plasma Physics* (Bristol: Institute of Physics Publishing)
[5] Shukla P K and Mamun A A 2003 *New J. Phys.* **5** 17
[6] Barkan A, Merlino RL and D'Angelo N 1995 *Phys. Plasmas* **2** 3563
[7] Thompson C, Barkan A, Merlino R L and D'Angelo N 1999 *IEEE Trans. Plasma Sci.* **27** 146
[8] Wang X, Bhattacharjee A and Hu S 2001 *Phys. Rev. Lett.* **86** 2569
[9] Murillo M S 2000 *Phys. Plasmas* **7** 33
[10] Pramanik J, Prasad G, Sen A and Kaw P K 2002 *Phys. Rev. Lett* **88** 175001
[11] Kaw P K and Sen A 1998 *Phys. Plasmas* **5** 3552
[12] Rosenberg M and Kalman G 1997 *Phys. Rev.* E **56** 7166
[13] Murillo M S 1998 *Phys. Plasmas* **5** 3116
[14] Shukla P K and Stenflo L 2003 *Phys. Lett.* A **315** 244
[15] Shukla P K and Mamun A A 2001 *IEEE Trans. Plasma Sci.* **29** 221
[16] Mamun A A, Eliasson B and Shukla P K 2004 *Phys. Lett.* A **332** 412
[17] Feldman W C *et al* 1983 *J. Geophys. Res.* **88** 96
[18] Lundlin R *et al* 1989 *Nature* **341** 609
[19] Futaana Y *et al* 2003 *J. Geophys. Res.* **108** 151
[20] Franz J R, Kintner P M and Pickett J S 1998 *Geophys. Res. Lett.* **25** 2041
[21] Xue J K 2003 *Phys. Lett.* A **314** 479
[22] Xue J K and He L 2003 *Phys. Plasmas* **10** 339
[23] Tian B and Gao Y T 2005 *Phys. Lett.* A **340** 243
[24] Ghosh S and Gupta M R 2005 *Phys. Plasmas* **12** 092306
[25] Ichimaru S, Iyetomi H and Tannaka S 1987 *Phys. Rep.* **149** 91
[26] Slattery W L, Doolen G D and DeWitt H E 1980 *Phys. Rev.* A **21** 2087
[27] Ghosh S 2004 *Phys. Plasmas* **11** 3602
[28] Melandsø F 1996 *Phys. Plasmas* **3** 3890
[29] Gill T S, Saini N S and Kaur H 2006 *Chaos Solitons Fractals* **28** 1106
[30] Wang Y Y and Zhang J F 2006 *Phys. Lett.* A **352** 155